

Astrophysical and Cosmological Constraints on Neutrino masses ¹

Kimmo Kainulainen ²

Theory Division, CERN, CH-1211, Geneva, Switzerland and
NORDITA, Blegdamsvej 17, DK-2100, Copenhagen Ø, Denmark

Keith A. Olive ³

Theoretical Physics Institute, School of Physics and Astronomy,
University of Minnesota, Minneapolis, MN 55455, USA

Abstract

We review some astrophysical and cosmological properties and implications of neutrino masses and mixing angles. These include: constraints based on the relic density of neutrinos, limits on their masses and lifetimes, BBN limits on mass parameters, neutrinos and supernovae, and neutrinos and high energy cosmic rays.

¹to appear in “Neutrino Mass”, Springer Tracts in Modern Physics, ed. by G. Altarelli and K. Winter.

²e-mail address: kimmo.kainulainen@cern.ch; Permanent address: University of Jyväskylä, Finland.

³e-mail address: olive@umn.edu

1 Introduction

The role of neutrinos in cosmology and astrophysics can not be understated [1]. They play a critical role in the physics of the early Universe, at temperatures scales of order 1 MeV, and strongly determine the abundances of the light elements produced in big bang nucleosynthesis. They almost certainly play a key role in supernova explosions, and if they have mass, could easily contribute to the overall mass density of the Universe. At the present time, the only indicators of neutrino masses are from astrophysical sources, the inferred neutrino oscillations of neutrinos produced in the Sun, and those produced in cosmic-ray collisions in the atmosphere. Indeed, their elusive character has proven that a great deal of information on neutrino properties can be gained by studying their behavior in astrophysical and cosmological environments. Here, we will try to elucidate some of these constraints on neutrino masses.

In our discussion below, we will assume that the early Universe is well described by a standard Friedmann-Lemaître-Robertson-Walker metric

$$ds^2 = dt^2 - R^2(t) \left[\frac{dr^2}{1 - kr^2} + r^2 (d\theta^2 + \sin^2 \theta d\phi^2) \right] \quad (1)$$

We further assume that thermal equilibrium was established at some early epoch and that we can describe the radiation by a black body equation of state, $p = \rho/3$ at a temperature T . Solutions to Einstein's equations allow one to determine the expansion rate of the Universe defined to be the Hubble parameter in terms of the energy density in radiation, the curvature and the cosmological constant. In the early Universe the latter two quantities can be neglected and we write

$$H^2 \equiv \left(\frac{\dot{R}}{R} \right)^2 = \frac{8\pi G_N \rho}{3} \quad (2)$$

where the energy density is

$$\rho = \left(\sum_B g_B + \frac{7}{8} \sum_F g_F \right) \frac{\pi^2}{30} T^4 \equiv \frac{\pi^2}{30} N(T) T^4 \quad (3)$$

The present neutrino contribution to the total energy density, relative to the critical density (for a spatially flat Universe) is

$$\Omega_\nu = \frac{\rho_\nu}{\rho_c} \quad (4)$$

where $\rho_c = 1.06 \times 10^{-5} h^2 \text{GeV}/\text{cm}^3$ and $h = H/100 \text{km}/\text{Mpc}/\text{s}$ is the scaled Hubble parameter. For a recent review of standard big bang cosmology, see [2].

2 The Cosmological Relic Density of Stable Neutrinos

The simplicity of the standard big bang model allows one to compute in a straightforward manner the relic density of any stable particle if that particle was once in thermal

equilibrium with the thermal radiation bath. At early times, neutrinos were kept in thermal equilibrium by their weak interactions with electrons and positrons. Equilibrium is achieved whenever some rate Γ is larger than the expansion rate of the Universe, or $\Gamma_i > H$. Recalling that the age of the Universe is determined by H^{-1} , this condition is equivalent to requiring that on average, at least one interaction has occurred over the life-time of the Universe. On dimensional grounds, one can estimate the thermally averaged low-energy weak interaction scattering cross section

$$\langle\sigma v\rangle\sim g^4T^2/m_W^4 \quad (5)$$

for $T \ll m_W$. Recalling that the number density scales as $n \propto T^3$, we can compare the weak interaction rate $\Gamma \sim n\langle\sigma v\rangle$, with the expansion rate given by eqs. (2) and (3). Neutrinos will be in equilibrium when $\Gamma_{\text{wk}} > H$ or

$$T^3 > \sqrt{8\pi^3 N/90} \, m_W^4/M_P \quad (6)$$

where $M_P = G_N^{-1/2} = 1.22 \times 10^{19}$ GeV is the Planck mass. For $N = 43/4$ (accounting for photons, electrons, positrons and three neutrino flavors) we see that equilibrium is maintained at temperatures greater than $\mathcal{O}(1)$ MeV (for a more accurate calculation see [3]).

The decoupling scale of $\mathcal{O}(1)$ MeV has an important consequence on the final relic density of massive neutrinos. Neutrinos more massive than 1 MeV will begin to annihilate prior to decoupling, and while in equilibrium, their number density will become exponentially suppressed. Lighter neutrinos decouple as radiation on the other hand, and hence do not experience the suppression due to annihilation. Therefore, the calculations of the number density of light ($m_\nu \lesssim 1$ MeV) and heavy ($m_\nu \gtrsim 1$ MeV) neutrinos differ substantially.

The number of density of light neutrinos with $m_\nu \lesssim 1$ MeV can be expressed at late times as

$$\rho_\nu = m_\nu Y_\nu n_\gamma \quad (7)$$

where $Y_\nu = n_\nu/n_\gamma$ is the density of ν 's relative to the density of photons, which today is 411 photons per cm^3 . It is easy to show that in an adiabatically expanding universe $Y_\nu = 3/11$. This suppression is a result of the e^+e^- annihilation which occurs after neutrino decoupling and heats the photon bath relative to the neutrinos. In order to obtain an age of the Universe, $t > 12$ Gyr, one requires that the matter component is constrained by

$$\Omega h^2 \leq 0.3. \quad (8)$$

From this one finds the strong constraint (upper bound) on Majorana neutrino masses: [4]

$$m_{\text{tot}} = \sum_\nu m_\nu \lesssim 28\text{eV}. \quad (9)$$

where the sum runs over neutrino mass eigenstates. The limit for Dirac neutrinos depends on the interactions of the right-handed states (see discussion below). As one can see, even

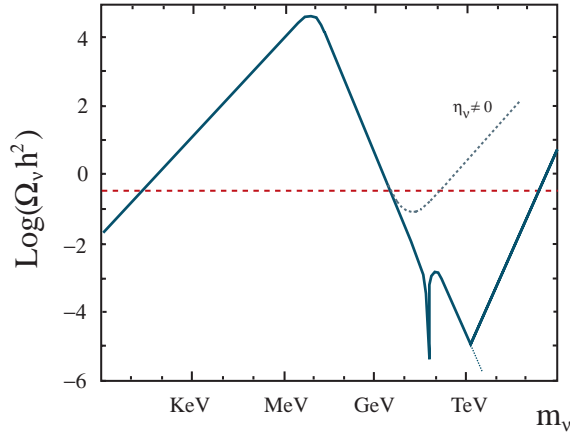


Figure 1: Summary plot of the relic density of Dirac neutrinos (solid) including a possible neutrino asymmetry of $\eta_\nu = 5 \times 10^{-11}$ (dotted).

very small neutrino masses of order 1 eV, may contribute substantially to the overall relic density. The limit (9) and the corresponding initial rise in $\Omega_\nu h^2$ as a function of m_ν is displayed in the Figure 1 (the low mass end with $m_\nu \lesssim 1$ MeV).

The calculation of the relic density for neutrinos more massive than ~ 1 MeV, is substantially more involved. The relic density is now determined by the freeze-out of neutrino annihilations which occur at $T \lesssim m_\nu$, after annihilations have begun to seriously reduce their number density [5]. The annihilation rate is given by

$$\Gamma_{ann} = \langle \sigma v \rangle_{ann} n_\nu \sim \frac{m_\nu^2}{m_Z^4} (m_\nu T)^{3/2} e^{-m_\nu/T} \quad (10)$$

where we have assumed, for example, that the annihilation cross section is dominated by $\nu\bar{\nu} \rightarrow f\bar{f}$ via Z -boson exchange¹ and $\langle \sigma v \rangle_{ann} \sim m_\nu^2/m_Z^4$. When the annihilation rate becomes slower than the expansion rate of the Universe the annihilations freeze out and the relative abundance of neutrinos becomes fixed. Roughly, $Y_\nu \sim (m \langle \sigma v \rangle_{ann})^{-1}$ and hence $\Omega_\nu h^2 \sim \langle \sigma v \rangle_{ann}^{-1}$, so that parametrically $\Omega_\nu h^2 \sim 1/m_\nu^2$. As a result, the constraint (8) now leads to a *lower* bound [5, 6, 7] on the neutrino mass, of about $m_\nu \gtrsim 3 - 7$ GeV, depending on whether it is a Dirac or Majorana neutrino. This bound and the corresponding downward trend $\Omega_\nu h^2 \sim 1/m_\nu^2$ can again be seen in Figure 1. The result of a more detailed calculation is shown in Figure 2 [7] for the case of a Dirac neutrino. The two curves show the slight sensitivity on the temperature scale associated with the quark-hadron transition. The result for a Majorana mass neutrino is qualitatively similar. Indeed, any particle with roughly weak scale cross-sections will tend to give an interesting value of $\Omega h^2 \sim 1$.

The deep drop in $\Omega_\nu h^2$, visible in Figure 1 at around $m_\nu = M_Z/2$, is due to a very strong annihilation cross section at Z -boson pole. For yet higher neutrino masses the

¹While this is approximately true for Dirac neutrinos, the annihilation cross section of Majorana neutrinos is p -wave suppressed and is proportional of the final state fermion masses rather than m_ν .

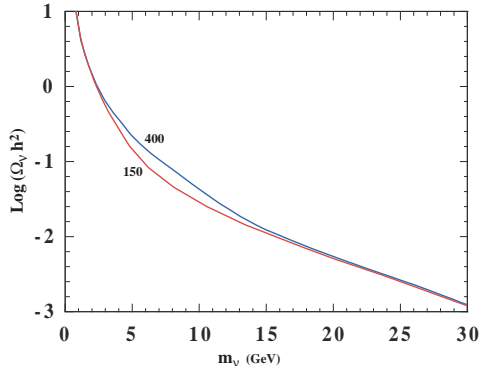


Figure 2: The relic density of heavy Dirac neutrinos due to annihilations [7]. The curves are labeled by the assumed quark-hadron phase transition temperature in MeV.

Z -annihilation channel cross section drops as $\sim 1/m_\nu^2$, leading to a brief period of an increasing trend in $\Omega_\nu h^2$. However, for $m_\nu \gtrsim m_W$ the cross section regains its parametric form $\langle\sigma v\rangle_{ann} \sim m_\nu^2$ due to the opening up of a new annihilation channel to W -boson pairs [8], and the density drops again as $\Omega_\nu h^2 \sim 1/m_\nu^2$. The tree level W -channel cross section breaks the unitarity at around $\mathcal{O}(\text{few})$ TeV [9] however, and the full cross section must be bound by the unitarity limit [10]. This behaves again as $1/m_\nu^2$, whereby $\Omega_\nu h^2$ has to start increasing again, until it becomes too large again at 200-400 TeV [10, 9] (or perhaps somewhat earlier as the weak interactions become strong at the unitarity breaking scale).

3 Neutrinos as Dark Matter

Based on the leptonic and invisible width of the Z boson, experiments at LEP have determined that the number of neutrinos is $N_\nu = 2.9841 \pm 0.0083$ [11]. Conversely, any new physics must fit within these brackets, and thus LEP excludes additional neutrinos (with standard weak interactions) with masses $m_\nu \lesssim 45$ GeV. Combined with the limits displayed in Figures 1 and 2, we see that the mass density of ordinary heavy neutrinos is bound to be very small, $\Omega_\nu h^2 < 0.001$ for masses $m_\nu > 45$ GeV up to $m_\nu \sim \mathcal{O}(100)$ TeV.

A bound on neutrino masses even stonger than Eqn. (9) can be obtained from the recent observations of active-active mixing in both solar- and atmospheric neutrino experiments. The inferred evidence for $\nu_\mu - \nu_\tau$ and $\nu_e - \nu_{\mu,\tau}$ mixings are on the scales $m_\nu^2 \sim 1 - 10 \times 10^{-5}$ and $m_\nu^2 \sim 2 - 5 \times 10^{-3}$. When combined with the upper bound on the electron-like neutrino mass $m_\nu < 2.8$ eV [12], and the LEP-limit on the number of neutrino species, one finds the constraint on the sum of neutrino masses:

$$0.05 \text{ eV} \lesssim m_{\text{tot}} \lesssim 8.4 \text{ eV}. \quad (11)$$

Conversely, the experimental and observational data then implies that the cosmological

energy density of all light, weakly interacting neutrinos can be restricted to the range

$$0.0005 \lesssim \Omega_\nu h^2 \lesssim 0.09. \quad (12)$$

Interestingly there is now also a lower bound due to the fact that at least one of the neutrino masses has to be larger than the scale $m^2 \sim 10^{-3} \text{ eV}^2$ set by the atmospheric neutrino data. Combined with the results on relic mass density of neutrinos and the LEP limits, the bound (12) implies that the ordinary weakly interacting neutrinos, once the standard dark matter candidate [13], can be ruled out completely as a dominant component of the dark matter.

This conclusion can be evaded if neutrinos are Dirac particles, and have a nonzero asymmetry however, since then the relic density could be governed by the asymmetry rather than by the annihilation cross section. Indeed, it is easy to see that the neutrino mass density corresponding to the asymmetry $\eta_\nu \equiv (n_\nu - n_{\bar{\nu}})/n_\gamma$ is given by [14]

$$\rho = m_\nu \eta_\nu n_\gamma, \quad (13)$$

which implies

$$\Omega_\nu h^2 \simeq 0.004 \eta_{\nu 10} (m_\nu / \text{GeV}). \quad (14)$$

where $\eta_{\nu 10} \equiv 10^{10} \eta_\nu$. We have shown the behaviour of the energy density of neutrinos with an asymmetry by the dotted line in the Figure 1. At low m_ν , the mass density is dominated by the symmetric, relic abundance of both neutrinos and antineutrinos which have already frozen out. At higher values of m_ν , the annihilations suppress the symmetric part of the relic density until $\Omega_\nu h^2$ eventually becomes dominated by the linearly increasing asymmetric contribution. In the figure, we have assumed an asymmetry of $\eta_\nu \sim 5 \times 10^{-11}$ for neutrinos with standard weak interaction strength. In this case, $\Omega_\nu h^2$ begins to rise when $m_\nu \gtrsim 20 \text{ GeV}$. Obviously, the bound (8) is saturated for $m_\nu = 75 \text{ GeV} / \eta_{\nu 10}$.

There are also other cosmological settings that give rise to interesting mass constraints on the eV scale. Indeed, light neutrinos were problematic in cosmology long before the improved mass limits leading to (12) were established, due to their effect on structure formation. Light particles which are still relativistic at the time of matter domination erase primordial perturbations due to free streaming out to very large scales [15]. Given a neutrino with mass m_ν , the smallest surviving non-linear structures are determined by the Jean's mass

$$M_J = 3 \times 10^{18} \frac{M_\odot}{m_\nu^2 (\text{eV})}. \quad (15)$$

Thus, for eV mass neutrinos the large scale structures, including filaments and voids [16, 17], must form first and galaxies whose typical mass scale is $\simeq 10^{12} M_\odot$ are expected to fragment out later. Particles with this property are termed hot dark matter (HDM). It seemed that neutrinos were ruled out because they tend to produce too much large scale structure [18], and galaxies formed too late [17, 19], at $z \leq 1$, whereas quasars and galaxies are seen out to redshifts $z \gtrsim 6$.

Subsequent to the demise of the HDM scenario, there was a brief revival for neutrino dark matter as part of a mixed dark matter model, using now more conventional cold dark

matter along with a small component of hot (neutrino) dark matter. The motivation for doing this was to recover some of the lost power on large scales that is absent in CDM models [20]. However, galaxies still form late in these models, and more importantly, almost all evidence now points away from models with $\Omega_m = 1$, and strongly favor models with a cosmological constant (Λ CDM).

Combining the rapidly improving data on key cosmological parameters with the better statistics from large redshift surveys has made it possible to go a step forward along this path. It is now possible to set stringent limits on the light neutrino mass density $\Omega_\nu h^2$, and hence on neutrino mass based on the power spectrum of the Ly α forest [21], $m_{\text{tot}} < 5.5$ eV, and the limit is even stronger if the total matter density, Ω_m is less than 0.5. This limit has recently been improved by the 2dF Galaxy redshift [22] survey by comparing the derived power spectrum of fluctuations with structure formation models. Focussing on the the presently favoured Λ CDM model, the neutrino mass bound becomes $m_{\text{tot}} < 1.8$ eV for $\Omega_m < 0.5$.

Finally, right handed or sterile neutrinos may also contribute to the dark matter. The mass limits for neutrinos with less than full weak strength interactions are relaxed [23]. For Dirac neutrinos, the upper limit varies between 100 – 200 eV depending on the strength of their interactions. For Majorana neutrinos, the limit is further relaxed to 200 – 2000 eV. This relaxation is primarily due to the dilution of the number density of super-weakly interacting neutrinos due to entropy production by decay and annihilation of massive states after their decoupling from equilibrium [24]. Such neutrinos make excellent warm dark matter candidates, albeit the viable mass range for galaxy formation is quite restricted [25].

4 Neutrinos and Big Bang Nucleosynthesis

Big bang nucleosynthesis is the cosmological theory of the origin of the light element isotopes D, ^3He , ^4He , and ^7Li [26]. The success of the theory when compared to the observational determinations of the light elements allows one to place strong constraints on the physics of the early Universe at a time scale of 1-100 seconds after the big bang. ^4He is the most sensitive probe of deviations from the standard model and its abundance is determined primarily by the neutron to proton ratio when nucleosynthesis begins at a temperature of ~ 100 keV (to a good approximation all neutrons are then bound to form ^4He). The ratio n/p is determined by the competition between the weak interaction rates which interconvert neutrons and protons,

$$p + e^- \leftrightarrow n + \nu_e, \quad n + e^+ \leftrightarrow p + \bar{\nu}_e, \quad n \leftrightarrow p + e^- + \bar{\nu}_e \quad (16)$$

and the expansion rate, and is largely given by the Boltzmann factor

$$n/p \sim e^{-(m_n - m_p)/T_f} \quad (17)$$

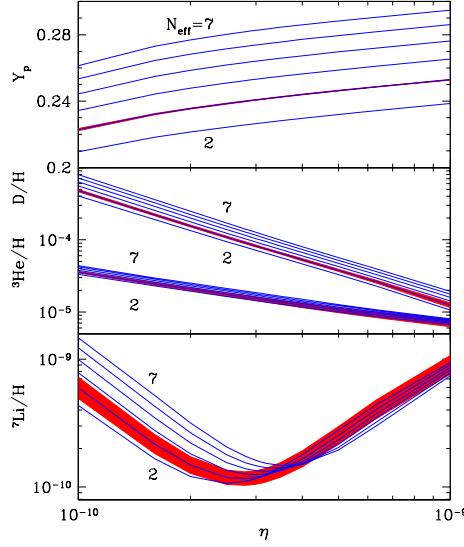


Figure 3: The light element abundances as a function of the baryon-to-photon ratio for different values of N_ν [27].

where $m_n - m_p$ is the neutron to proton mass difference. As in the case of neutinos discussed above, these weak interactions also freeze out at a temperature of roughly 1 MeV when

$$G_F^2 T_f^5 \sim \Gamma_{\text{wk}}(T_f) = H(T_f) \sim \sqrt{G_N N} T_f^2 \quad (18)$$

The freeze-out condition implies the scaling $T_f^3 \sim \sqrt{N}$. From Eqs. (17) and (18), it is then clear that changes in N , caused for example by a change in the number of light neutrinos N_ν , would directly influence n/p , and hence the ^4He abundance. The dependence of the light element abundances on N_ν is shown in Figure 3 [27], where plotted is the mass fraction of ^4He , Y , and the abundances by number of the D , ^3He , and ^7Li as a function of the baryon-to-photon ratio, η , for values of $N_\nu = 2 - 7$. As one can see, an upper limit to Y , combined with a lower limit to η will yield an upper limit to N_ν [28].

Assuming no new physics at low energies, the value of η is the sole input parameter to BBN calculations. It is fixed by the comparison between BBN predictions and the observational determinations of the isotopic abundances [29]. From ^4He and ^7Li , one finds a relatively low value [30, 29] for $\eta \sim 2.4 \times 10^{-10}$ corresponding to a low baryon density $\Omega_B h^2 = 0.009$ with a 95% CL range of 0.006 – 0.017. Deuterium, on the other hand, implies a large value of η and hence a large baryon density: $\eta \sim 5.8 \times 10^{-10}$ and $\Omega_B h^2 \sim 0.021$ with a 95% CL range of 0.018 – 0.027. The value of the baryon density has also been determined recently from measurements of microwave background anisotropies. The recent result from DASI [31] indicates that $\Omega_B h^2 = 0.022^{+0.004}_{-0.003}$, while that of BOOMERanG-98 [32], $\Omega_B h^2 = 0.021^{+0.004}_{-0.003}$ (using 1σ errors).

With the value of η fixed, one can use He abundance measurements to set limits on

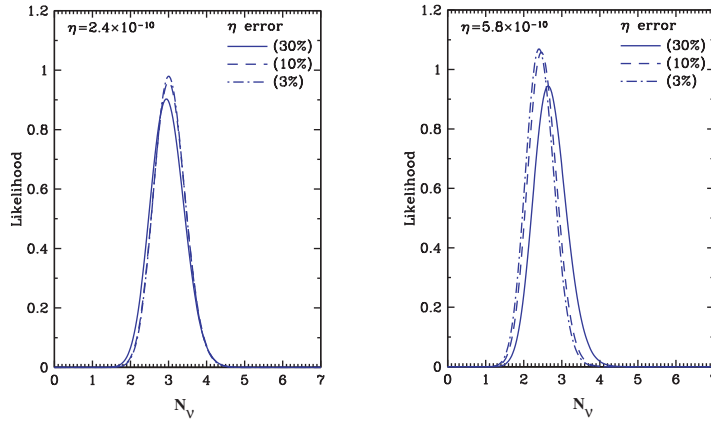


Figure 4: (a) The distribution in N_ν assuming a value of $\eta = 2.4 \times 10^{-10}$ from ^4He and ^7Li and the CBI measurement of the microwave background anisotropy [27]. The curves show the effect of the expected increased accuracy in the CMB determination of η . (b) As in (a), but assuming a value of $\eta = 5.8 \times 10^{-10}$ from D and the DASI and BOOMERanG measurements of the microwave background anisotropy.

new physics. In particular one can set upper limits the number of neutrino flavors. Taking $Y_p = 0.238 \pm 0.002 \pm 0.005$ (see e.g. [33]), we show in Figure 4 the likelihood functions for N_ν based on both the low and high values of η [27]. The curves show the impact of an increasingly accurate determination of η from 30% to 3%. If one assumes a 20% uncertainty in η (the current uncertainty level), these calculations provide upper limits of

$$\begin{aligned} N_\nu &< 3.9 & \eta &= 2.4 \times 10^{-10} \\ N_\nu &< 3.6 & \eta &= 5.8 \times 10^{-10} \end{aligned} \quad (19)$$

at the 95% CL. Although, as noted above, LEP has already placed very stringent limit to N_ν , the limit (19) is useful, because it actually applies to the total number of new particle degrees of freedom and is not tied specifically to neutrinos. In fact, more generally, the neutrino limit can be translated into a limit on the expansion rate of the Universe at the time of BBN, which can be applied to a host of other constraints on particle properties.

4.1 BBN limits on Neutrino masses and lifetimes

As discussed above, the nucleosynthesis prediction for light element abundances is sensitive to the changes in the expansion rate of the universe, which depends on the energy density of the universe during the BBN era (2). This extra energy density could be in the form of new massless degrees of freedom, in which case their number is directly constrained by equation (19). Equally well the extra energy density could reside in the form of massive long lived but unstable neutrinos, in which case nucleosynthesis provides interesting constraints on their masses and life-times.

We already pointed out that the relic density of neutrinos strongly depends on whether

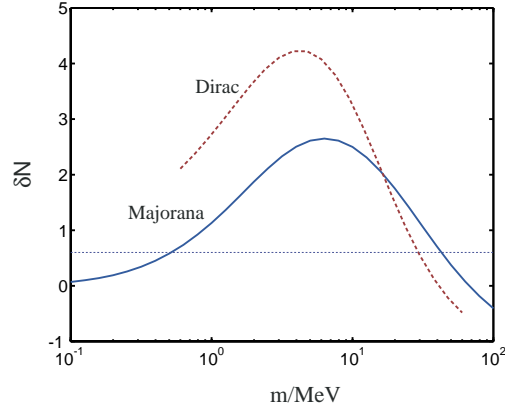


Figure 5: Plot of the effective number of neutrino degrees of freedom during BBN for a Dirac (dashed) and a Majorana neutrino (solid) [35].

they decouple while relativistic or nonrelativistic. Here the calculations also depend on how the neutrino life-times relate to the BBN time-scale of about 100 seconds. Also, in order to get reliable results for the light element abundances, one must keep track of the induced perturbations (electron neutrino heating) in the weak reaction rates (16) in addition to computing changes in the expansion rate. Nevertheless, even in this case it is customary to measure the change in helium abundance in units of equivalent effective neutrino degrees of freedom N_{eff} , such that the limit (19) can be applied on $N_{\text{eff}}(\Delta Y(m_\nu, \tau_\nu))$.

When the neutrino life-time is much larger than 100 seconds, neutrinos are effectively stable on a nucleosynthesis scale [34, 35, 36]. While accounting for changes in the rates in Eq. (16) is important for the detailed bounds, the bulk behaviour of $N_{\text{eff}}(m_\nu)$ is dictated by the neutrino mass contribution to the energy density. Obviously, when $m_\nu \ll 0.1$ MeV, neutrinos are effectively massless during BBN, and $N_{\text{eff}}(m_\nu) \rightarrow 3$ when $m_\nu \rightarrow 0$. For masses in excess of 0.1 MeV, but below the neutrino decoupling temperature of $\mathcal{O}(\text{few})$ MeV, their number density is unsuppressed and their mass density can be large during BBN, causing N_{eff} to increase. For yet larger masses however, the Boltzmann factor shown in (10) begins to suppress the mass density and eventually turns N_{eff} down again. This behaviour is shown in Figure 5 for a massive Dirac and Majorana type tau-neutrino [35]. The bound (19) yields an excluded region for stable neutrino masses centered around $\mathcal{O}(\text{few})$ MeV. For $N_\nu < 3.6$ the lower bound is $m_\nu > 42$ MeV (Majorana) and $m_\nu > 30$ MeV (Dirac) [35]. This is only relevant for ν_τ , and is complementary to the present laboratory limit on the τ -like neutrino, $m_\nu < 18$ MeV [38]. Due to contributions from pion decays and inverse decays to neutrinos, the upper bound from BBN depends on the QCD-phase transition temperature, T_{QCD} , and is also different for τ - and μ -neutrinos because of their different scattering rates off muons. Imposing again the constraint $N_\nu < 3.6$, and taking $T_{\text{QCD}} = 200$ MeV gives [39]:

$$m_\nu \lesssim 230 \text{ KeV} \quad \mu - \text{like}$$

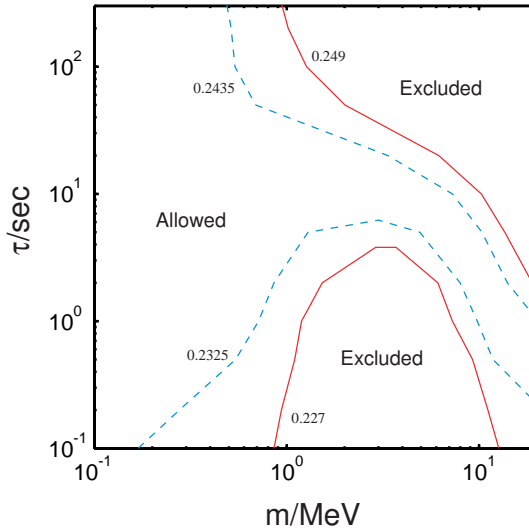


Figure 6: Plot of BBN-constraint on masses and life-times of an unstable tau neutrino. Contours are labeled by one (dashed) and two sigma (solid) deviations from the observed value of Y_p . The upper right corner is excluded due to too much and the lower part of the graph by too little ${}^4\text{He}$ being produced.

$$m_\nu \lesssim 290 \text{ KeV} \quad \tau - \text{like.} \quad (20)$$

The laboratory limit on the muon-like neutrino, for comparison, is $m_\nu \lesssim 170 \text{ keV}$ [40]. To improve this, the BBN limit should be improved to $N_\nu \lesssim 3.4$ [39].

When the neutrino life-time is small or comparable to the nucleosynthesis time scale, one has to account for neutrino decay processes as well. This involves solving for the distributions of the final state decay products, which might include new particles like majorons, and their possible direct effect on BBN. (For example energetic photons would cause the dissociation of the newly generated light nuclei.) Such calculations have been done by many groups [41, 42], and the results are given in exclusion plots in the mass-vs-life-time plane. Constraints are possible for masses of order $\mathcal{O}(1)$ MeV and life-times of order $\mathcal{O}(1)$ second. In Figure 6, we show a constraint on tau-neutrino masses and life-times as an example (data taken from the reference [42]).

4.2 BBN limits on Neutrino mixing parameters

Despite losing the competitive edge *w.r.t.* masses and life-times, BBN continues to put interesting limits on other neutrino mass parameters, relevant for neutrino oscillations. Indeed, the LEP-limit of course only applies to neutrinos with weak interactions, while neutrinos without weak interactions, or *sterile* neutrinos, have been proposed in many different contexts over the years. At present, a prime motivation to introduce sterile neutrinos is to explain the LSND neutrino anomaly [43] in conjunction with the solar and atmospheric neutrino deficits.

BBN on the other hand is sensitive to any type of energy density changing the expansion rate in the $\mathcal{O}(0.1\text{-}1)$ MeV range, irrespective of their interactions. It is therefore very interesting to observe that even if no sterile neutrinos were created at very early times, they could be excited by mixing effects in the early universe prior to nucleosynthesis. The basic mechanism is very simple. Suppose that an active state ν_α ($\alpha = e, \mu, \tau$) *mixes* with a sterile state ν_s . That is, the neutrino mass matrix and hence the Hamiltonian, is not diagonal in the interaction bases. The mixing is further affected by the forward scattering interactions with the background plasma, felt by the active state. As a result, even though a neutrino state was initially produced in purely active projection, after some time t it has become some coherent linear combination of both active and sterile states:

$$\nu(t) = c_e(t)\nu_e + c_s(t)\nu_s. \quad (21)$$

The coherent evolution of this state is interrupted by collisions, which effect a sequence of quantum mechanical measurements of the flavour content of the propagating state. Since the sterile state has no interactions, each measurement is complete, and collapses the wave-function to the sterile state with a probability $P_{\nu_e \rightarrow \nu_s}(t) = |c_s(t)|^2$. As a result, the sterile states are populated roughly with an average rate

$$\Gamma_{\nu_s} = \Gamma_\nu \langle |c_s(t)|^2 \rangle_{\text{coll}} = \frac{1}{2} \sin^2 2\theta_m \Gamma_{\nu_\alpha}. \quad (22)$$

where Γ_{ν_α} is the weak interaction rate of the active state ν_α , and we have assumed that the oscillation time is short in comparison with the collision time scale. The matter mixing angle θ_m is given by [44]

$$\sin^2 2\theta_m = \frac{\sin^2 2\theta_0}{1 - 2\chi \cos 2\theta_0 + \chi^2} \quad (23)$$

where $\sin 2\theta_0$ is the mixing angle in vacuum and $\chi \equiv 2p|V|/\delta m^2$ where δm^2 is the mass squared difference of the vacuum mass eigenstates, $p \sim T$ is the momentum and $|V|$ is the matter induced effective potential to the Hamiltonian [45, 44]. The weak rate scales as $\Gamma_{\nu_\alpha} \sim T^5$. Moreover $\chi \sim T^6$ at very high temperatures, which causes a strong matter suppression for mixing and hence $\Gamma_{\nu_s} \sim T^{-7}$. At very small temperatures $\theta_m \rightarrow \theta_0$ on the other hand, and hence $\Gamma_{\nu_s} \sim T^5$. The rate is thus suppressed both at very large and at very small temperatures [46]. In the intermediate region of $\mathcal{O}(\text{few})$ MeV however, Γ_{ν_s} can exceed the expansion rate bringing a significant amount of sterile neutrinos into equilibrium. An accurate treatment of the problem requires a numerical solution of the appropriate quantum kinetic equations, and the results depend on whether the mostly active state is heavier ($\delta m^2 < 0$) or lighter ($\delta m^2 > 0$) of the mixing states. We show the results of such a calculation in Figure 7 below [44]. The lines are labeled by constant effective number of degrees of freedom during BBN: $\delta N_\nu \equiv N_\nu - 3$. The most recent limits corresponding to (19) can be interpolated from the curves shown. It is the area above the curves which is excluded by BBN-limit.

The BBN-limit can be converted to an upper bound on the sterile neutrino flux [47] in the atmospheric and the solar neutrino observations. Using $N_\nu < 3.6$ one finds

$$\sin^2 \theta_{\mu s} \lesssim 0.03 \quad (\text{Atmospheric})$$

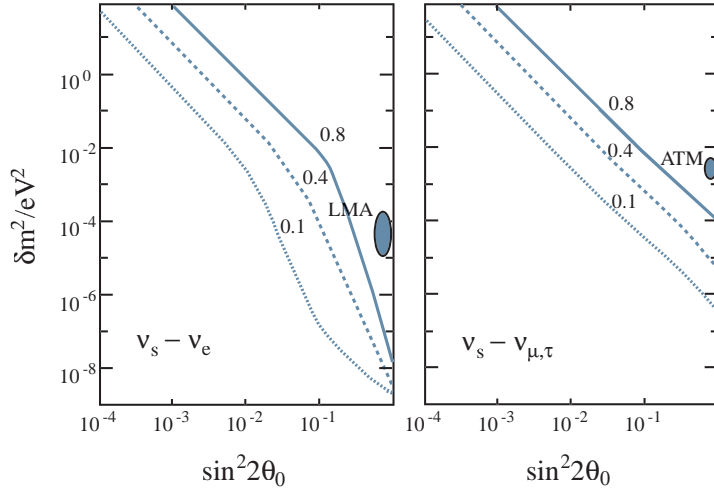


Figure 7: Plotted are the BBN constraints on the active sterile neutrino mixing parameters [44] for $\nu_\alpha = \nu_e$ (left) and $\nu_\alpha = \nu_{\mu,\tau}$ (right). Regions to the right from the contours labeled by the bound on effective neutrino degrees of freedom $\delta N_{\text{eff}} = N_{\text{eff}} - 3$ are excluded. Shown are also the current regions corresponding to active-sterile mixing parameters for atmospheric (ATM) and the large mixing angle (LMA) solar neutrino solutions.

$$\sin^2 \theta_{\text{es}} \lesssim 0.06 \quad (\text{Solar LMA}), \quad (24)$$

whereas the bounds from the atmospheric and solar neutrino experiments are about an order of magnitude weaker: $\sin^2 \theta_{\mu s} \lesssim 0.48$ and $\sin^2 \theta_{\text{es}} \lesssim 0.72$.

The constraints shown in the Figure 7 and in Equation (24) depend on the assumption that the primordial lepton asymmetry is not anomalously large [48]. In ref. [49] it was suggested that a large effective asymmetry violating this assumption could actually be generated by oscillations given a particular neutrino mass and mixing hierarchy. For a while these ideas generated a lot of interest, as they would have allowed reconciling all observed anomalies (including LSND) with the nucleosynthesis constraints. However, in these scenarios at least one of the active states would have to be much heavier than the two others, which is not allowed by the atmospheric and solar neutrino flux observations. As a result, the bounds (24) hold, and in particular nucleosynthesis is very much at odds with the possible existence of the LSND-type sterile state. To see this, observe that creating a large enough effective mixing between $\bar{\nu}_\mu$ and $\bar{\nu}_e$ to explain the anomaly [43] would require a sterile intermediate with $m_{\nu_s} \simeq 1$ eV, and $\sin^2 2\theta_{\mu e} \simeq \frac{1}{2} \sin^2 2\theta_{\mu s} \sin^2 2\theta_{se} \gtrsim 10^{-2} (\delta m^2 / \text{eV}^2)^{-2}$. In other words at least one of the active-sterile mixings should satisfy $\sin^2 2\theta_{(\mu,e)s} \gtrsim 0.15 (\delta m^2 / \text{eV}^2)^{-1}$, which is well within the BBN excluded regions shown in Figure 7. (It would be excluded even by $N_{\text{eff}} \lesssim 3.9$, although we do not show that contour in Figure 7).

It should finally be noted that only the active-sterile type oscillations are cosmologically interesting, since active-active type oscillations have hardly any effect on the expansion

rate or the weak interaction rates [50].

5 Neutrinos and Supernovae

Neutrinos have for long been known to play important role in the physics of supernovae. To be sure, it is clear that by far the largest part, roughly 99%, of the gravitational binding energy of about 3×10^{53} erg involved in the explosion of a type II supernova is carried out by neutrinos, while just 1% powers the shock wave responsible for blowing out the mantle of the star, and only a tiny fraction of about 0.1% escapes in the form of light responsible for the spectacular sights observed in the telescopes watching the sky.

The formation of the neutrino burst in the collapse of a type II supernova is rather well understood. The temporal structure of the burst and the energy spectrum of the emitted neutrinos can be computed fairly well [51]. Existing or planned large scale neutrino detectors [53] can be used to observe deviations from these signatures and to obtain interesting information on neutrino masses and mixing parameters [52], given a future observation of a Galactic supernova. We show an example of a compilation of neutrino fluxes and spectra in Figure 8.

A number of constraints on new physics and in particular on neutrino parameters have already been deduced from the famous SN1987A event in the Small Magellanic Cloud. Of these, perhaps the most direct is the upper bound on the neutrino mass derivable from the maximum duration of the observed duration of the neutrino pulse of about 10 seconds. Given the initial energy spectrum of neutrinos and the distance to the supernova, one can compute the expected spread in the arrival times of the neutrinos to earth as a function of neutrino mass. Comparing the predictions with the observations has been shown to yield the bound [54]

$$m_{\nu_e} \lesssim 6 - 20 \text{ eV}. \quad (25)$$

The observed pulse length also lends to the classic *cooling argument*: any new physics that would enhance the neutrino diffusion such that the cooling time drops below the observed duration, must be excluded. Cooling arguments have been used to set limits on various neutrino properties [55] such as active-sterile neutrino mixing [56] and neutrino magnetic moments. The magnetic dipole moment bound in particular was recently revised by Ayala et al. [57] to

$$\mu_{\nu_e} \lesssim 1 - 4 \times 10^{-12} \mu_B \quad (26)$$

which is a couple of orders of magnitude more stringent than the best laboratory bounds, and comparable to the bound coming from the globular cluster red giant cooling arguments [58], which give $\mu_{\nu_e} \lesssim 3 \times 10^{-12} \mu_B$.

At present, most of the activity concerning neutrinos in supernovae has focussed on the effects of neutrino transport in supernova explosion dynamics rather than with finding constraints on neutrino mixing parameters or masses. Indeed, the details of the physics responsible for the actual visibly observed supernova explosion, including blowing out the stellar mantle, are not very well understood. In particular, the shock wave, which forms

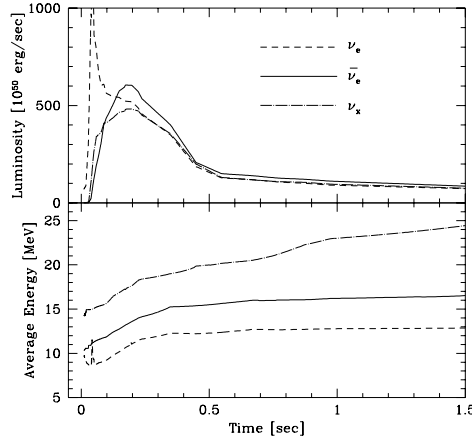


Figure 8: Time evolution of neutrino luminosities and average energies: ν_x represents the spectrum of ν_μ , ν_τ , $\bar{\nu}_\mu$ and $\bar{\nu}_\tau$. Figure taken from [53].

deep within the iron core as the infall of matter is reversed due to the stiffening of the nuclear matter equation of state, is typically found to be too weak to explode the star. This is believed to be due to energy loss from the shock and dissociating iron nuclei on its way out from the core to the mantle. In the popular “delayed explosion scenario”, the stalling shock wave is rejuvenated by energy transfer to the shock from the huge energy-flux of neutrinos free streaming away from the core. Recent numerical simulations including diffusive neutrino transport do not verify this expectation however [59]; while neutrinos definitely help, they do not appear to solve the problem. These results are not conclusive because the diffusive transport equations used so far [59] did not include all relevant neutrino interactions, most notably the nuclear brehmsstrahlung processes [60, 51]. Furthermore, processes other than diffusive processes, such as convective flows in the core and behind the shock, appear to play an important role as well [61].

It is of course possible that a successful SN explosion requires help of some new physics to channel energy more efficiently to the shock, and neutrino-oscillations have already been considered for this role [62]. The idea is that ν_μ and ν_τ , interact more weakly and hence escape more energetic from deeper in the core than do electron neutrinos. Arranging mixing parameters so that $\nu_{\mu,\tau}$ turn resonantly to ν_e in the mantle behind the shock could increase the energy deposited to the shock significantly. Unfortunately the mass difference needed for the resonant transition would be very big:

$$\delta m^2 \sim 2E\nu_{\text{eff}} \simeq 1.5 \times 10^5 \rho_e E_\nu^{100} \text{ eV}^2 \quad (27)$$

where ρ_e is the electron density in units 10^{10} g/cm³, which at the shock front is about 10^{-3} , and E_ν^{100} is the neutrino energy in units of 100 MeV. So one gets $m_\nu \gtrsim 10$ eV, which is excluded by the present data. A similar idea was behind the suggestion [63], that neutrino magnetic moments induce resonant transitions from ν_R (which escape energetic from deep in the core) to ν_L behind the mantle. This mechanism could actually be used to evade the

bound (26), but as it demands a magnetic moment of order $\mu_\nu \sim 10^{-11} \mu_B$ it has problems in coping with the red giant cooling bound [58].

Sterile neutrinos could also be relevant for supernovae by alleviating the problems with the r-process nucleosynthesis, which is thought to be responsible for creation of the most heavy elements. In the standard SN calculations the r-process nucleosynthesis is not effective due to too efficient de-neutronization by the processes $\nu_e + n \rightarrow e^- + p$. If electron neutrinos mixed with a sterile state however, these processes could be made less effective, increasing the neutron density in the mantle, and hence improving the r-process efficiency [64].

Finally, there is also the old problem of the “kick”-velocities of pulsars (neutron star remnants of supernova explosions). It has proven difficult to arrange for these velocities, which average around 450 km/sec, based on the normal fluid dynamics in asymmetrical SN-explosions. The momentum carried out by neutrinos $p_\nu \simeq E_\nu$, on the other hand, is about 100 times larger than the pulsar kinetic energy, so that a mere one per cent asymmetry in the neutrino emission would be enough to power the pulsar velocities. Interesting attempts have been made to explain such asymmetric emission by an asymmetric distribution of inhomogeneities in the SN magnetic fields, combined with a large neutrino magnetic moment [63], or just the magnetic field induced deformation of the neutrino spheres [65]. However, the former would again need probably too large magnetic moment to work, and a detailed analysis of the latter [66] shows that the asymmetric flux is very suppressed, requiring unrealistically large magnetic fields in excess of $10^{17} G$. The quest for the explanation of pulsar velocities is still on, and neutrino solution still looks appealing from the pure energetics point of view.

Before we conclude this section, we would like to mention, several other astrophysical limits on neutrino properties. A sure limit to the mean life/mass ratio is obtained from solar x- and γ - ray fluxes [67]. The limit is $\tau/m_{\nu_1} > 7 \times 10^9$ s/eV. This is far superior to the laboratory bound of 300 s/eV [68]. Other much stronger limits ($> O(10^{15})$ s/eV) are available from the lack of observation of γ -rays in coincidence with neutrinos from SN 1987A [69]. This latter limit applies to the heavier neutrino mass eigenstates, ν_2 and ν_3 , as well.

6 Neutrinos and Cosmic Rays

One of the most interesting puzzles in astrophysics today concerns the observations of ultra high energy cosmic rays (UHECR), beyond the so called Greisen-Zatsepin-Kuzmin (GZK) cutoff

$$E_{\text{GZK}} \simeq 5 \times 10^{19} \text{ eV}. \quad (28)$$

The problem is that cosmic rays at these energies necessarily need to be of extragalactic origin, since their gyromagnetic radius within the galactic magnetic field far exceeds galactic dimensions. Yet, the attenuation lengths of both protons and photons are rather small in comparison with intergalactic distances, and neither can have originated by fur-

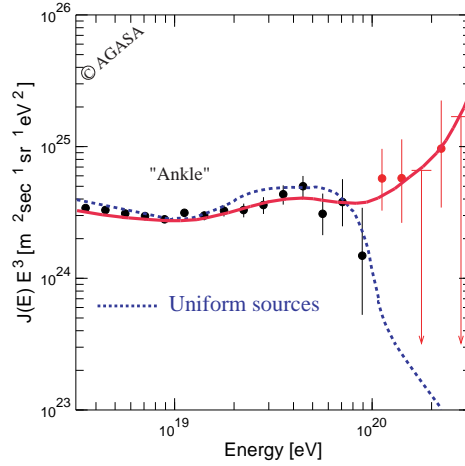


Figure 9: Scaled by E^3 spectrum of highest energy cosmic rays near the GZK cutoff. The dotted line corresponds to the expectation from uniformly distributed extragalactic sources, and the solid line shows the prediction of a Z-burst model of ref. [72]. (Figure modified from the original found at the AGASA web page [71].)

ther than about 50 Mpc away from us, due to their scattering off the intergalactic cosmic photon background. As a result, one would expect that the cosmic ray spectrum would abruptly end around $E \sim E_{\text{GZK}}$ due to scattering off of the microwave background. This cutoff is represented by the dotted line in Figure 9. In contrast, several groups, most notably the HiRes [70] and AGASA [71] collaborations, have reported events with energies well above the GZK-cutoff: the latest compilation of AGASA, for example, contains 10 events above the scale $E > 10^{20}$ eV, observed since 1993.

The origin of UHECR's has been the subject of lively discussions over the last few years. Apart from having astrophysical origins, being accelerated in extreme environments at extragalactic distances (in AGN's, GRB's or Blazars), they have been attributed to the decay products of very heavy particles or of topological defects. All these explanations have problems, however. Astrophysical explanations face the difficult task of accelerating particles to the extreme energies required, with little or no associated sub-TeV-scale photonic component (as none have been ever observed). This is in addition to the above mentioned problem of the propagation of UHECR's over extragalactic distances. Decay explanations are somewhat disfavoured by the growing evidence of doublets and triplets in AGASA data, and by the correlation between the UHECR arrival directions with far compact Blazars [73], which appear rather to be pointing towards astrophysical origin.

The attenuation problem for extragalactical UHECR's can be avoided however, if they cross the universe in the form of a neutrino beam, since neutrinos travel practically free over super-Hubble distances. Indeed, should this be the case, the initial ν_{UHE} 's could occasionally interact with the cosmological relic neutrino background close to us, giving rise to "Z-bursts" of hadrons and photons [74], which then would give rise to the observed UHECR events. Indeed, given a neutrino mass m_ν , such a collision has sufficient CM-

energy for resonant Z production if

$$E_\nu = \frac{M_Z^2}{2m_\nu} \simeq 4.2 \times 10^{21} \text{eV} \left(\frac{\text{eV}}{m_\nu} \right). \quad (29)$$

The requirement of super-GZK-energies for the initial ν_{UHE} beam leads immediately to the interesting mass scale for neutrinos: $m_\nu \sim \mathcal{O}(1)$ eV.

Z -burst models have been extensively studied lately [75]. For example, in ref. [72] it was shown that a Z -burst model with $m_\nu = 0.07$ eV, corresponding to a degenerate neutrino spectrum, could reproduce the AGASA-data including the spectral features, such as the “ankle” and the “bump” observed at $E \lesssim E_{\text{GZK}}$. The best fit model of ref. [72] is shown by the solid line in Figure 9. While the agreement with AGASA data is good, it should be noted that this model predicts that cosmic ray primaries are exclusively photons above $E \gtrsim 10^{20}$ eV, whereas the $E \simeq 3 \times 10^{20}$ eV event observed by Fly’s Eye is almost certainly not caused by a photon [76]. The model also predicts a large increase of the cosmic ray flux above $\text{few} \times 10^{20}$ eV (as a direct result of the huge initial energy needed: $E_{\nu_{\text{UHE}}} \simeq 6 \times 10^{22}$ eV), which exacerbates the already outstanding problem of the origin of UHECR’s. These problems could be ameliorated by assuming somewhat larger neutrino masses, and it has been argued by Fodor *et al.* [75], that the Z -burst scenario can already be used to *constrain* the mass, plausibly to within $m_\nu \sim 0.08 - 1.3$ eV, in very good agreement with other mass determinations. The analysis of ref. [75], was restricted to Z -resonance interactions however, while for higher CM-energies the cross section [8] for pair production of gauge bosons $\nu\nu \rightarrow ZZ, WW$ becomes important. These reactions have been shown to give acceptable solutions with larger neutrino masses $m_\nu \gtrsim 3$ eV [77].

In summary, although the origin of UHECR’s remains a mystery today, it is almost certain that if it has to do with extragalactic sources, neutrino physics plays a very important role in the interpretation of these events.

Acknowledgments

K.K. would like to thank Steen Hannestad and Petteri Keranen for useful advice. The work of K.A.O. was supported partly by DOE grant DE-FG02-94ER-40823.

References

- [1] A. D. Dolgov, arXiv:hep-ph/0202122.
- [2] K. Olive and J.A. Peacock, to appear in the Review of Particle Properties, 2002.
- [3] K. Enqvist, K. Kainulainen and V. Semikoz, Nucl. Phys. B **374**, 392 (1992).
- [4] R. Cowsik and J. McClelland, Phys. Rev. Lett. **29**, 669 (1972); A.S. Szalay and G. Marx, Astron. Astrophys. **49**, 437 (1976)
- [5] P. Hut, Phys. Lett. B**69**, 85 (1977); B.W. Lee and S. Weinberg, Phys. Rev. Lett. **39**, 165 (1977)
- [6] E.W. Kolb and K.A. Olive, Phys. Rev. **D33**, 1202 (1986); E: **34**, 2531 (1986)
- [7] R. Watkins, M. Srednicki and K.A. Olive, Nucl. Phys. **B310**, 693 (1988).
- [8] K. Enqvist, K. Kainulainen and J. Maalampi, Nucl. Phys. B **317**, 647 (1989).
- [9] K. Enqvist and K. Kainulainen, Phys. Lett. B **264**, 367 (1991).
- [10] K. Griest and M. Kamionkowski, Phys. Rev. Lett. **64**, 615 (1990).
- [11] D. Abbaneo *et al.* [ALEPH Collaboration], arXiv:hep-ex/0112021.
- [12] Ch. Weinheimer, et al, Phys. Lett. B**460** (1999) 219.
- [13] D.N. Schramm and G. Steigman, Ap. J. **243** (1981) 1.
- [14] P. Hut, K.A. Olive, Phys. Lett. B**87** (1979) 144.
- [15] J.R. Bond, G. Efstathiou and J. Silk, Phys. Lett. **45** (1980) 1980; Ya.B. Zeldovich and R.A. Sunyaev, Sov. Ast. Lett. **6** (1980) 457.
- [16] P.J.E. Peebles, Ap. J. **258** (1982) 415; A. Melott, M.N.R.A.S. **202** (1983) 595; A.A. Klypin, S.F. Shandarin, M.N.R.A.S. **204** (1983) 891.
- [17] C.S. Frenk, S.D.M. White and M. Davis, Ap. J. **271** (1983) 417.
- [18] S.D.M. White, C.S. Frenk and M. Davis, Ap. J. **274** (1983) 61.
- [19] J.R. Bond, J. Centrella, A.S. Szalay and J. Wilson, in *Formation and Evolution of Galaxies and Large Structures in the Universe*, ed. J. Andouze and J. Tran Thanh Van, (Dordrecht-Reidel 1983) p. 87.
- [20] M. Davis, F. J. Summers and D. Schlegel, Nature **359** (1992) 393; A. Klypin, J. Holtzman, J. Primack and E. Regos, Astrophys. J. **416**, 1 (1993).

- [21] R. A. Croft, W. Hu and R. Dave, Phys. Rev. Lett. **83**, 1092 (1999) [arXiv:astro-ph/9903335].
- [22] ØElgarøy et. al. , [arXiv:astro-ph/0204152].
- [23] K. A. Olive and M. S. Turner, Phys. Rev. D **25**, 213 (1982).
- [24] G. Steigman, K. A. Olive and D. N. Schramm, Phys. Rev. Lett. **43** (1979) 239; K. A. Olive, D. N. Schramm and G. Steigman, Nucl. Phys. B **180**, 497 (1981).
- [25] S. H. Hansen, J. Lesgourgues, S. Pastor and J. Silk, [arXiv:astro-ph/0106108].
- [26] K. Olive, G. Steigman, and T.P. Walker, Phys. Rep. **333**, 389 (2000); B.D. Fields and S. Sarkar, to appear in the Review of Particle Properties, 2002.
- [27] R. H. Cyburt, B. D. Fields and K. A. Olive, Astropart. Phys. **17**, 87 (2002) [arXiv:astro-ph/0105397].
- [28] G. Steigman, D.N. Schramm, and J. Gunn, Phys. Lett. **B66**, 202 (1977)
- [29] R.H. Cyburt, B.D. Fields, and K.A. Olive, New Astron. **6**, 215 (2001)
- [30] B. D. Fields, K. Kainulainen, K. A. Olive and D. Thomas, New Astron. **1**, 77 (1996).
- [31] C. Pryke et al., Ap. J. **568**, 46 (2002), [arXiv:astro-ph/0104490]
- [32] C.B. Netterfield et al., (2001), [arXiv:astro-ph/0104460]
- [33] B.D. Fields and K.A. Olive, Astrophys. J. **506**, 177 (1998); A. Peimbert, M. Peimbert, and V. Luridiana, Ap. J. **565**, 668 (2002), [arXiv:astro-ph/0107189]
- [34] E. W. Kolb, M. S. Turner, A. Chakravorty and D. N. Schramm, Phys. Rev. Lett. **67**, 533 (1991).
- [35] B. D. Fields, K. Kainulainen and K. A. Olive, Astropart. Phys. **6**, 169 (1997); K. Kainulainen, in Neutrino physics and astrophysics 1996, Helsinki, Finland [arXiv:hep-ph/9608215].
- [36] S. Hannestad and J. Madsen, Phys. Rev. Lett. **76**, 2848 (1996) [Erratum-ibid. **77**, 5148 (1996)];
- [37] A. D. Dolgov, S. H. Hansen and D. V. Semikoz, Nucl. Phys. B **524** (1998) 621.
- [38] L. Passalacqua, Nucl. Phys. Proc. Suppl. **55C** (1997) 435.
- [39] A. D. Dolgov, K. Kainulainen and I. Z. Rothstein, Phys. Rev. D **51**, 4129 (1995).
- [40] K. Assamagan, et al, Phys. Rev. D **53** (1996) 6065.

- [41] M. Kawasaki, P. Kernan, H. S. Kang, R. J. Scherrer, G. Steigman and T. P. Walker, Nucl. Phys. B **419**, 105 (1994); S. Dodelson, G. Gyuk and M. S. Turner, Phys. Rev. D **49**, 5068 (1994); S. Hannestad, Phys. Rev. D **57** (1998) 2213.
- [42] A. D. Dolgov, S. H. Hansen, S. Pastor and D. V. Semikoz, Nucl. Phys. B **548** (1999) 385.
- [43] A. Aguilar et al, Phys. Rev. D **64** (2001) 112007.
- [44] K. Enqvist, K. Kainulainen and M. J. Thomson, Nucl. Phys. B **373**, 498 (1992).
- [45] D. Notzold and G. Raffelt, Nucl. Phys. B **307**, 924 (1988).
- [46] K. Kainulainen, Phys. Lett. B **244**, 191 (1990).
- [47] K. Kainulainen and A. Sorri, JHEP **0202**, 020 (2002).
- [48] K. Enqvist, K. Kainulainen and J. Maalampi, Phys. Lett. B **244**, 186 (1990).
- [49] R. Foot and R. R. Volkas, Phys. Rev. Lett. **75**, 4350 (1995); R. Foot, M. J. Thomson and R. R. Volkas, Phys. Rev. D **53**, 5349 (1996).
- [50] P. Langacker, S. T. Petcov, G. Steigman and S. Toshev, Nucl. Phys. B **282** (1987) 589.
- [51] G. G. Raffelt, [arXiv:astro-ph/0105250].
- [52] A. S. Dighe and A. Y. Smirnov, Phys. Rev. D **62**, 033007 (2000).
- [53] T. Totani, K. Sato, H. E. Dalhed and J. R. Wilson, Astrophys. J. **496**, 216 (1998).
- [54] T. J. Loredo and D. Q. Lamb, Ann. N.Y. Acad. Sci. **571** (1989) 601; Phys. Rev. D **65**, 063002 (2002).
- [55] G. Raffelt, Ann. Rev. Nucl. Part. Sci. **49** (1999) 163.
- [56] D. Notzold, Phys. Lett. B **196**, 315 (1987). K. Kainulainen, J. Maalampi and J. T. Peltoniemi, Nucl. Phys. B **358** (1991) 435.
- [57] A. Ayala, J. C. D’Olivo and M. Torres, Phys. Rev. D **59** (1999) 111901.
- [58] G. G. Raffelt, Phys. Rept. **320** (1999) 319.
- [59] M. Rampp and H. T. Janka, Astrophys. J. **539** (2000) L33; [arXiv:astro-ph/0005438]. M. Liebendorfer et al, Phys. Rev. D **63**, 103004 (2001).
- [60] S. Hannestad and G. Raffelt, Astrophys. J. **507** (1998) 339.
- [61] G. G. Raffelt, arXiv:hep-ph/0201099.

- [62] G. M. Fuller et al, *Astrophys. J.* **389** (1992) 517.
- [63] M. B. Voloshin, *Phys. Lett. B* **209** (1988) 360.
- [64] C. J. Horowitz, [arXiv:astro-ph/0108113] (2002); Y.-Z. Qian, [arXiv:astro-ph/0203194] (2002).
- [65] A. Kusenko and G. Segre, *Phys. Rev. Lett.* **77**, 4872 (1996).
- [66] H. T. Janka and G. G. Raffelt, *Phys. Rev. D* **59**, 023005 (1999) [arXiv:astro-ph/9808099].
- [67] G. G. Raffelt, *Phys. Rev. D* **31** (1985) 3002.
- [68] F. Reines, H. W. Sobel and H. S. Gurr, *Phys. Rev. Lett.* **32** (1974) 180.
- [69] F. Von Feilitzsch and L. Oberauer, *Phys. Lett. B* **200** (1988) 580. E. L. Chupp, W. T. Vestrand and C. Reppin, *Phys. Rev. Lett.* **62** (1989) 505. E. W. Kolb and M. S. Turner, *Phys. Rev. Lett.* **62**, 509 (1989). S. A. Bludman, *Phys. Rev. D* **45** (1992) 4720.
- [70] D. J. Bird et al. [HIRES Collaboration], *Astrophys. J.* **424** (1994) 491.
- [71] M. Takeda et al., *Phys. Rev. Lett.* **81** (1998) 1163. The AGASA home page: www.akeno.icrr.u-tokyo.ac.jp/AGASA/
- [72] G. Gelmini and G. Varieschi, arXiv:hep-ph/0201273.
- [73] P. G. Tinyakov and I. I. Tkachev, *JETP Lett.* **74** (2001) 445.
- [74] T. J. Weiler, *Astropart. Phys.* **11** (1999) 303.
- [75] Z. Fodor, S. D. Katz and A. Ringwald, arXiv:hep-ph/0203198.
- [76] See for example, F. Halzen, [arXiv:astro-ph/0111059].
- [77] D. Fargion, P. G. De Sanctis Lucentini, M. Grossi, M. De Santis and B. Mele, arXiv:hep-ph/0112014; D. Fargion, B. Mele and A. Salis, *Astrophys. J.* **517** (1999) 725.